Magnetic correlations and their dependence on excess oxygen in $La_2NiO_{4+\delta}$

T. Freltoft
Corporate R&D, NKT, DK-2605 Brondby, Denmark

D. J. Buttrey
Department of Chemical Engineering, Colburn Laboratory, University of Delaware, Newark, Delaware 19716

G. Aeppli
AT&T Bell Laboratories, 600 Mountain Avenue, Murray Hill, New Jersey 07974

D. Vaknin
Physics Department, Riso National Laboratory, DK-4000 Roskilde, Denmark

G. Shirane
Brookhaven National Laboratory, Upton, New York 11973
(Received 20 May 1991)

We report results of elastic- and inelastic-neutron-scattering studies of three single crystals of the layered perovskite $La_2NiO_{4+\delta}$, with $\delta=0.00$, 0.067, and 0.077, as well as neutron powder diffraction on a material with an oxygen excess $\delta\approx0.065$. The magnetic correlations are highly sensitive to the oxygen content, and three-dimensional antiferromagnetic order sets in at $T_N\geq300$ K, and $T_N=68$, and 48 K for the single crystals, respectively, and at $T_N=74$ K for the powder sample. The crystal with $\delta=0.067$ was studied in detail to characterize the tetragonal to orthorhombic ($T_s=232$–240 K) and antiferromagnetic ($T_N=68$ K) transitions. The order parameter $\eta(T)$ for the orthorhombic distortion shows a power-law dependence on temperature with the exponent $\beta=0.21$ and hysteresis, suggesting that this transition is less than second order. Two-dimensional critical scattering is observed around the antiferromagnetic phase transition. The magnetic excitation spectra in the three-dimensional ordered state are characterized by small anisotropy gaps between ~0 and 3 meV, and large effective in-plane spin-wave velocities, which decrease with increasing δ. For $\delta=0.077$, $c\approx130$ meV Å; and for $\delta=0.00$, $c\geq300$ meV Å.

I. INTRODUCTION

The layered perovskite La_2NiO_4 is isostructural with the parent high-T_c superconductor, La_2CuO_4, and has been extensively studied because of its unusual transport and magnetic properties. Early investigations showed clear inconsistencies due to lack of control of oxygen stoichiometry, on which structure and properties are sensitively dependent. Since Ni^{2+} ($3d^8$) has spin $S=1$ in contrast with Cu^{2+} ($3d^9$) with spin $S=\frac{1}{2}$ for La_2CuO_4, a study of magnetic correlations in $La_2NiO_{4+\delta}$ as a function of oxygen nonstoichiometry may provide useful insight into possible magnetic aspects of the mechanism for high-T_c superconductivity in the analogous cuprates.

Early reports[1–5] consistently concluded that the La_2NiO_4 structure was of the undistorted body-centered tetragonal K_2NiF_4 type with $I4/mmm$ (No. 139) (Ref. 6) symmetry, but a comparison of lattice constants revealed discrepancies which we now attribute to variations in oxygen stoichiometry. Subsequent electron-diffraction studies revealed superstructure reflections consistent with a distortion associated with octahedral rotation.[7] From a combination of electron diffraction and x-ray powder diffraction, a $\sqrt{2}\mathbf{a}\times\sqrt{2}\mathbf{b}\times\mathbf{c}$ supercell with orthorhombic *Bmab* (No. 64) symmetry was identified for nearly stoichiometric material at room temperature.[8,9] Odier *et al.*[10] investigated the temperature dependence of cell constants of several powder specimens quenched from 1000°C in atmospheres ranging from pure argon to air. They found tetragonal $I4/mmm$ symmetry for more oxidized compositions and orthorhombic symmetry for samples quenched under argon. Variations in stoichiometry in the $La_2NiO_{4+\delta}$ system have been shown to arise from incorporation of interstitial oxygen defects in samples where the [La]/[Ni] ratio was found to be 2.00 ± 0.01, using standard wet chemical methods.[11]

Odier *et al.*[12] reported the symmetry of the stoichiometric composition as orthorhombic *Pncb* (No. 50) for stoichiometric La_2NiO_4 based on powder x-ray and neutron data; however, the neutron Rietveld refinement of $La_2NiO_{4.00}$ by Jorgenson *et al.*,[13] as well as recent results from four-circle x-ray diffraction on a transparent single-domain crystal of stoichiometric La_2NiO_4 (Ref. 14) are consistent with *Bmab* symmetry at room temperature. X-ray single-crystal refinement[14] of the orthorhombic *Bmab* phase gave an octahedral polar canting angle of 5.4° with $r_{Ni\text{-}O}=1.948$ Å in the basal plane and 2.244 Å axially (Fig. 1). Lattice parameters were found to be $a=5.473$ Å, $b=5.532$ Å, and $c=12.541$ Å. Jorgenson *et al.*[13] also found that the or-

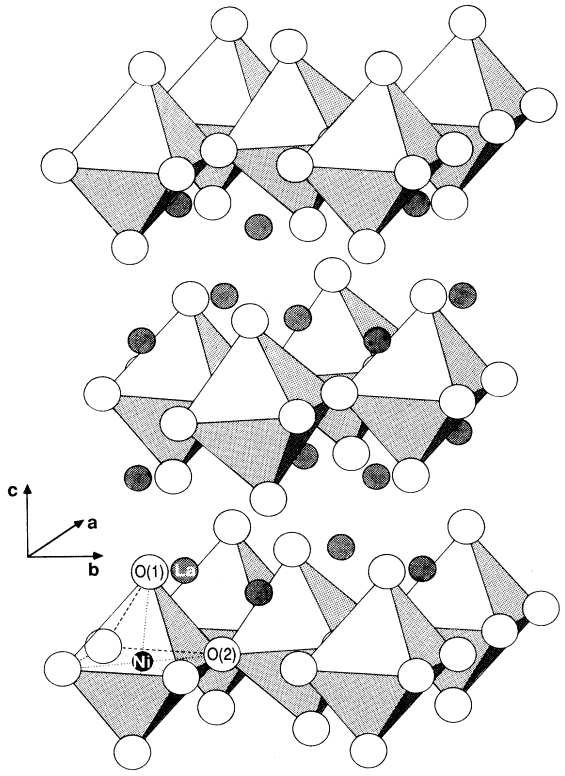

FIG. 1. Clinographic projection of the orthorhombic *Bmab* structure of stoichiometric La_2NiO_4 from Ref. 14.

thorhombic *Bmab* phase exists for $La_2NiO_{4+\delta}$ in the range $0<\delta<0.02$, whereas an oxygen-rich phase exists for $0.13<\delta<0.18$ with *Fmmm* symmetry rather than *I4/mmm*. For intermediate stoichiometries, the two phases were found to coexist, suggesting that phase separation has occured similar to that observed in the $La_2CuO_{4+\delta}$ system[15]. The oxygen defect was located at the $(\frac{1}{4},\frac{1}{4},\frac{1}{4})$ site by neutron Rietveld refinement of the *Fmmm* phase.[13]

Tavares[16] reported differential scanning calorimetric results showing a broad anomaly in the temperature range 570–680 K, which is attributed to a second-order structural transition. On heating, electron diffraction[8] shows a gradual loss of superlattice reflections in stoichiometric La_2NiO_4 in the range 550-700 K, consistent with a continuous orthorhombic to tetragonal (*I4/mmm*) transition. Rodriguez-Carvajal *et al.*[17] report a second phase transition near 80 K in stoichiometric La_2NiO_4 with no obvious change of space group, but with basal plane lattice parameters of the low-temperature phase which are equivalent. Lander *et al.*[18] have recently found that this is a first-order transition occurring at 70.0 ± 0.5 K for $\delta=0.001$–0.002 and have assigned the symmetry of the low-temperature phase as $P4_2/ncm$.

The phonon dispersion curves of La_2NiO_4 have been measured by Pintschovius *et al.*[19] using inelastic neutron scattering. They found pronounced anomalies in the phonon branches involving in-plane nickel-oxygen stretching vibrations. Boni *et al.*[20] did not feel that they could observe similar anomalies in recent neutron experiments on La_2CuO_4.

Early transport measurements on nonstoichiometric, polycrystalline La_2NiO_4 showed semiconducting behavior at low temperature and a gradual change to metallic behavior above 500 K.[21,22] Single-crystal transport measurements[7,9] on $La_2NiO_{4+\delta}$ with $0.02<\delta<0.05$ show that this transition is restricted to the basal planes, with no anomaly evident with current directed along the unique, higher resistivity axis. The anisotropy approaches 2 orders of magnitude at low temperature. Odier *et al.*[23] report more insulating behavior in a stoichiometric sample. The temperature dependence has been described as Arrhenius-like[7,9] with activation energies in the range 50–80 meV, or in terms of Mott variable-range hopping.[23]

The magnetic susceptibility, $\chi(T)$, is also strongly dependent on δ. Highly stoichiometric La_2NiO_4 shows nearly temperature-independent behavior in the range 80 K–475 K.[8,9,24] Higher-temperature Faraday measurements by Schartman and Honig[25] indicate that $T_N=650$ K near the stoichiometric limit. Susceptibility measurements on powders prepared by high-temperature syntheses in air typically show a small cusp or break in $\chi(T)$ near 200 K.[26,27] A pronounced cusp in $\chi(T)$ is observed in single crystals near 200 K with $\delta\simeq0.02$ for $\mathbf{H}\|\mathbf{c}$, yet unobserved with $\mathbf{H}\perp\mathbf{c}$; a smaller anomaly is observed at lower temperatures for larger δ.[8,24] These anomalies have been interpreted in terms of the onset of three-dimensional (3D) antiferromagnetic order with spins slightly canted out of the basal plane, producing a net moment along **c** in the presence of an applied field,[8,9,24] much as has been subsequently proposed for $La_2CuO_{4+\delta}$.[28,29]

Spin-wave dispersions in the antiferromagnetically ordered phase of $La_2CuO_{4+\delta}$ are very difficult (but not impossible) to probe because of the extremely high-spin-wave velocities found in these materials, $c\simeq0.85$ eV Å.[30] In $La_2NiO_{4+\delta}$, however, much lower spin-wave velocities (0.1–0.2 eV Å) have been observed[31] and are strongly dependent on δ. In a recent letter,[31] two of us reported elastic- and inelastic-neutron-scattering experiments on two single crystals of $La_2NiO_{4+\delta}$.

In the present paper we describe a detailed neutron-scattering study of the magnetic correlations in three single crystals and one polycrystalline sample of $La_2NiO_{4+\delta}$ with $\delta=0.00$, 0.067, 0.077, and ~0.065, respectively. The experimental procedure is described in Sec. II. In Sec. III, we discuss the overall structural properties based on neutron powder and single-crystal diffraction of the respective phases, and we look in detail at the orthorhombic-tetragonal transition of one of the single crystals. Section IV concentrates on the magnetic phase transition and its oxygen-defect dependence, and Sec. V is concerned with the spin-wave dynamics as a function of oxygen content. Finally, in Sec. VI, we summarize the results and compare with results known for La_2CuO_4.

II. EXPERIMENTAL METHODS

A. Sample preparation and characterization

The $La_2NiO_{4+\delta}$ single crystals investigated were grown by radio-frequency skull melting, as described in Ref. 32. For the present study, three single crystals denoted LN1, LN2, and LN3 were used, where LN signifies lanthanum nickel (oxide). Crystal LN1, with an approximate volume of 1.0 cm^3, was annealed at 1470 K in a CO/CO_2 buffer to achieve an oxygen fugacity, $\log_{10} f_{O_2} = -8.70$, as monitored by a Y-$ZrO_2$ solid electrolyte cell calibrated against the NiO/Ni buffer. The La_2NiO_4/Ni reduction boundary at 1470 K occurs at approximately $\log_{10} f_{O_2} = -9.0$. Since the range of substoichiometric compositions is expected to be very small, requiring Ni^+ for charge compensation, the most stoichiometric ($\delta = 0$) composition for La_2NiO_4 is expected very near the reduction boundary. Crystals LN2 and LN3 are as-grown crystals with volumes of approximately 0.5 cm^3 selected from different regions of the 1.4 kg boule in which they were grown.

The amount of interstitial oxygen was determined for crystals LN2 and LN3 by multiple iodometric titrations carried out in a glove box under nitrogen with deaerated solutions, yielding $\delta = 0.067$ and 0.077 ± 0.002, respectively. The value of δ for the powder specimen was not directly determined; however, based on comparison of lattice parameters T_N and T_s between powder and single-crystal specimens determined as described below, we infer that $\delta \approx 0.065$. Room-temperature x-ray powder diffraction patterns were acquired with a Philips APD 3520 diffractometer equipped with a Johansson graphite monochromator on the detector arm, using Cu $K\alpha$ radiation. Fragments from crystals LN2 and LN3 were ground with Si internal standards to determine room-temperature lattice constants.

B. Neutron scattering

Neutron powder diffraction was carried out on a 10-g sample, which was obtained by grinding as-grown crystals of irregular shape which were not well suited for other use. To minimize variations in δ, these crystals were selected from a localized region near the center of the boule. The sample was sealed in helium and mounted in a closed-cycle refrigerator on the H4S spectrometer at Brookhaven's High Flux Beam Reactor. A neutron wavelength of 2.37 Å was used along with a set of pyrolytic graphite filters capable of discriminating to better than 1 part in 10^4 against the $\lambda/2$ component of the beam.

The single-crystal experiments were conducted on several triple-axis spectrometers at Brookhaven's High Flux Beam Reactor. For the unpolarized experiments, pyrolytic graphite crystals were used as monochromator and analyzer with fixed final energies $3.5 \leq E_f \leq 50$ meV, and different combinations of 10′ to 80′ collimators depending on the conflicting requirements of intensity and resolution. The higher-order neutrons were always attenuated by pyrolytic graphite or cooled Be filters. The polarized neutron experiments discussed in Secs. IV and VI were performed on a modified triple-axis spectrometer using vertically magnetized Heusler $Cu_2MnAl(111)$ transmission crystals as monochromator and analyzer. For the measurements below room temperature, the samples were mounted in $(h0l)$ and $(hk0)$ zones (using *Bmab* notation) on the cold finger of a closed-cycle displex refrigerator.

III. STRUCTURE

There are several possible subgroups of the idealized K_2NiF_4 structure—$I4/mmm$ (No. 139) which may arise as a consequence of displacive phase transitions generating $\sqrt{2} \times \sqrt{2} \times 1$ supercells.[6] These supercells are expected to belong to the subgroups *Bmab* (No. 64), $P4_2/ncm$ (No. 138), or *Pccn* (No. 56). *Fmmm* symmetry may also be observed if there is significant disorder in the NiO_6 octahedral distortions. In the case of *Bmab*, the stoichiometric La_2NiO_4 space group at room temperature, octahedral rotation occurs about the **a** axis, whereas in $P4_2/ncm$ rotation about $\langle 1\bar{1}0 \rangle$ is observed. In the case of *Pccn*, the rotation would occur about an axis intermediate between $\langle 100 \rangle$ and $\langle 1\bar{1}0 \rangle$. For reference, the room-temperature symmetry of stoichiometric La_2CuO_4 is *Bmab* while oxygen excess $La_2CuO_{4+\delta}$ has been described as possessing *Bmab* (Ref. 33) or *Fmmm* (Ref. 15) symmetry.

A. Powder diffraction

Room-temperature x-ray powder diffraction patterns from powdered fragments from crystals LN2 and LN3 are consistent with single-phase $I4/mmm$ symmetry. Lattice parameters for LN2 are $a = 3.8689(2)$ Å and $c = 12.6248(10)$ Å based on high-angle reflections. For LN3, $a = 3.8685(2)$ Å and $c = 12.6353(6)$ Å.

The neutron powder diffraction pattern for $La_2NiO_{4+\delta}$($\delta \approx 0.065$) at room temperature is also consistent with a single-phase tetragonal $I4/mmm$ structure with $a = 3.871(4)$ Å and $c = 12.630(5)$ Å. Although no evidence of other phases was observed, the R factor of a preliminary powder refinement is limited to about 12%, probably due to disorder associated with either a correlated distribution of interstitial oxygen or octahedral tilting. As the sample was cooled, significant broadening of the (110) tetragonal peak was observed in the range 220–250 K, indicative of a transition to an orthorhombic phase. At 9 K the powder diffraction pattern corresponds to orthorhombic *Bmab* with $a = 5.452(2)$ Å, $b = 5.490(2)$ Å, and $c = 12.617(2)$ Å. The splitting of the (400), (040) reflections at 9 K is shown in Fig. 2, corresponding to a splitting parameter $(b - a/a)_0 = 0.007$.

B. Single-crystal diffraction

Crystal LN2 with $\delta = 0.067$ was studied in detail by neutron diffraction in the temperature region around the orthorhombic-to-tetragonal transition. This was done on the cold source spectrometer (H9) with an incident neutron energy of 3.5 meV and very tight collimation in or-

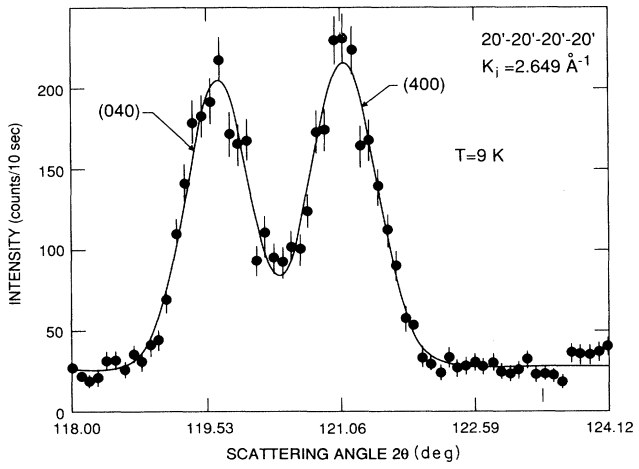

FIG. 2. Splitting of the (400) and (040) reflections at $T=10$ K for the polycrystalline sample with $\delta \approx 0.065$.

der to resolve the splitting of the (200), (020) reflections of the *Bmab* cell as close to the transition as possible. These reflections are observed as a sum of (200) and (020) due to twinning of the crystal. The temperature dependence of the reflections was examined both on heating and cooling to check for hysteresis. A sum of two Gaussians was fitted to each scan, from which **a** and **b** were obtained. The temperature dependencies of **a** and **b** are plotted for heating and cooling in Fig. 3(a). The splitting parameter is plotted as a function of temperature in Fig. 3(b). It is clear that the transition is hysteretic with $T_S^{\downarrow}=232.2$ K and $T_S^{\uparrow}=240.5$ K. The solid curve in Fig. 3(b) represents a power-law fit to the data for decreasing temperature, from which the exponent obtained is $\eta=0.21$. The relatively small exponent and hysteresis suggest that the transition is less than second order. Crystal LN3 with $\delta=0.077$ exhibited broadening of reflections at low temperatures, as expected due to orthorhombic distortion; however, the splitting parameter was too small to clearly resolve the structural transition with the available resolution.

IV. MAGNETIC ORDERING

All of the $La_2NiO_{4+\delta}$ samples investigated exhibit 3D antiferromagnetic (AFM) order below some temperature $T_N < T_S$, where T_S is the onset temperature for the tetragonal-orthorhombic transition. T_N depends strongly on the oxygen nonstoichiometry, δ, as is also observed in La_2CuO_4.[34]

A. Powder diffraction

Below 75 K, the powder sample exhibits reflections in addition to the *Bmab*-allowed reflections (h,k,l). Because their intensities decay with increased scattering angle, they originate from magnetic order. Figure 4 shows a 2θ scan near the (011) and (101) peak positions (indicated by arrows) at 9 and 103 K demonstrating loss of 3D AFM order at the higher temperature. The resolution

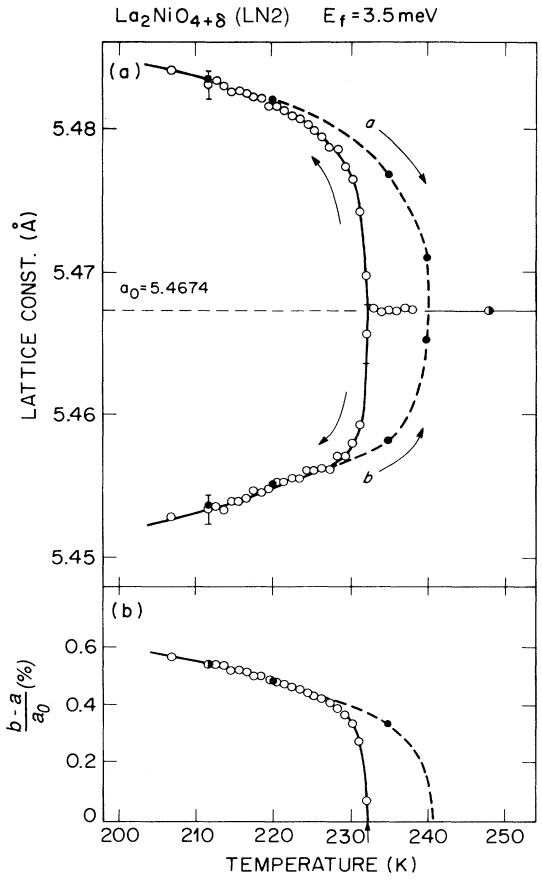

FIG. 3. Temperature dependence of (a) the basal plane lattice parameters, a and b, and (b) the orthorhombic splitting parameter, $(b-a)/a_0$, of crystal LN2.

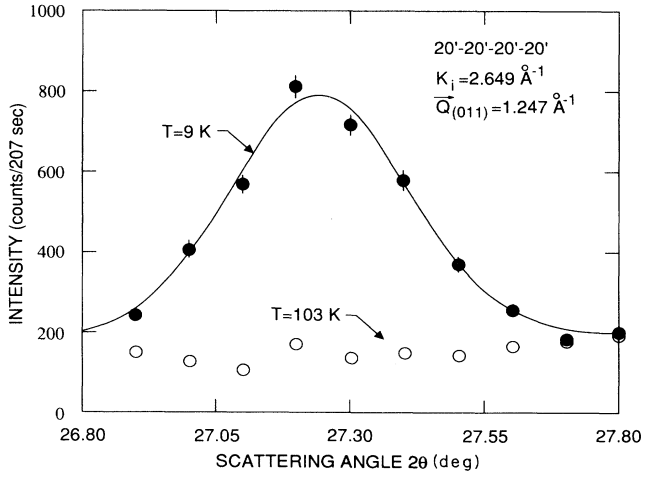

FIG. 4. A 2θ scan of the (011) magnetic reflection of the polycrystalline sample ($\delta \approx 0.065$) at $T=9$ and 103 K.

was sufficient to show that the superlattice peak is at the (011) and not the (101) position, which means that the antiferromagnetic order propagates along [100], not [010]. The systematic absence of reflections such as (100) implies that the magnetic moments are parallel to [100]. Thus, the magnetic structure consists of AFM-ordered basal planes which are stacked so that nearest-neighbor Ni^{2+} ions are oppositely polarized as illustrated in Fig. 6(a). This is distinguished from the magnetic structures found in K_2NiF_4 (Ref. 35) and La_2CuO_4 (Ref. 36) [Fig. 6(b)] where moments are ordered along [001] and [100], respectively. Table I summarizes the results for the ordered moments [in the structure of Fig. 6(a)] obtained from analyzing various powder reflections. The ordered moment at 9 K was determined to be $0.86\mu_B$ using the form-factor data of NiO.[37]

Figure 5 shows the normalized intensity temperature dependence of the magnetic peak (011), characteristic of a continuous transition. The fitted curve is of the form $I \sim (1-T/T_N)^{\beta}$, where $T_N = 74 \pm 2$ K and $\beta = 0.27 \pm 0.05$. The meaning of the parameter β is unclear, however, because of the obvious disorder in this nonstoichiometric sample.

B. Single-crystal diffraction

Below T_N, superlattice reflections were observed at $(0kl)$ positions where both k and l are odd and at $(h0l)$ positions with h odd and $l \neq 0$ even. Polarized neutron diffraction confirmed these to be of magnetic origin and verified the direction of ordered moments as [100]. Not surprisingly, these reflections are consistent with those found in the powder and associated with the structure of Fig. 6(a). The peak intensity of the (011) reflection is presented as a function of temperature in Fig. 5(b) for crystals LN2 and LN3. These curves exhibit considerable rounding, most probably due to disorder in these $\delta \neq 0$ samples relative to what is seen in typical antiferromagnets. If we define them as the onset temperatures for visible AFM Bragg scattering, the Néel temperatures for these crystals are 68 and 48 K, respectively.

C. Critical scattering from single crystal

$La_2NiO_{4+\delta}$ also exhibits strong two-dimensional magnetic correlations between spins in the basal plane for $T > T_N$,[31] similar to those observed in La_2CuO_4,[38] which are characterized by the presence of rods of inelastic scattering along the $[10l]$ and $[01l]$ directions. The correlations are dynamic in character, with no statically

TABLE I. The ordered magnetic moment, μ, of $La_2NiO_{4.065}$ at 10 K determined from the magnetic reflections, assuming the magnetic structure of Fig. 6(a), using the Ni form factor from Ref. 37.

hkl	O (Å^{-1})	$(\sin\theta)/\lambda$	μ/μ_B
011	1.247	0.10	0.86(5)
102	1.524	0.12	0.86(6)
013	1.884	0.15	0.85(5)

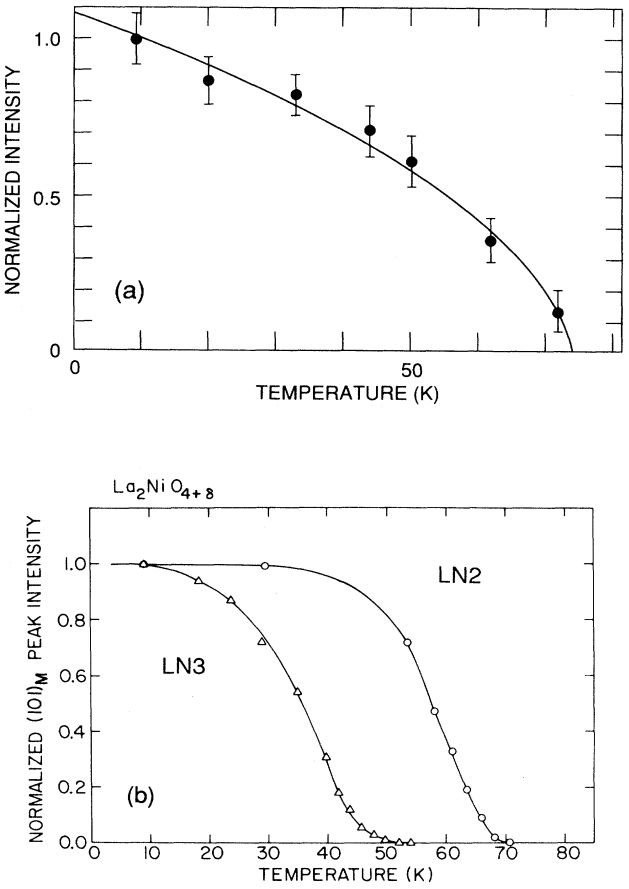

FIG. 5. Temperature dependence of the normalized intensity of the (011) magnetic reflection for (a) the $\delta \approx 0.065$ powder sample, and (b) for crystals LN2 and LN3.

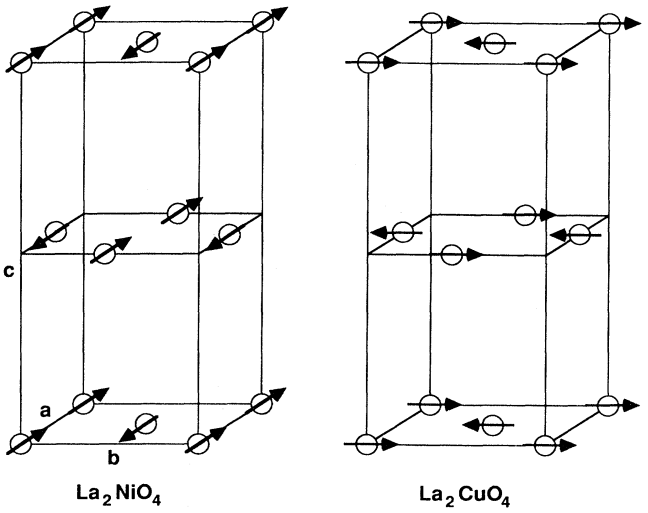

FIG. 6. A comparison of the 3D magnetic structures of La_2NiO_4 and La_2CuO_4 for $T < T_N$. Note that the orientation of crystallographic axes is matched to Fig. 1 for comparison.

ordered moment; therefore, the rods are not easily seen for the elastic-scattering condition $\hbar\omega=0$, but only when the cross section is integrated over energy.[31,39] As the 3D ordering temperature, T_N, is approached, two-dimensional quasielastic critical scattering begins to appear near $\hbar\omega=0$. Figure 7 shows the temperature dependence of the nominal $\hbar\omega=0$ peak intensity at a representative point along the rod, $\mathbf{Q}=(1,0,1.2)$ for crystal LN2. The quasielastic scattering exhibits a very pronounced peak near the Néel point, $T_N=68$ K.

To further investigate the quasielastic scattering in crystal LN2, energy scans were obtained at four different temperatures near T_N. Figure 8 shows scans obtained with the scattering vector held fixed at $\mathbf{Q}=(1,0,1.2)$ and the quasielastic incoherent background subtracted using equivalent scans obtained off the rod at $\mathbf{Q}=(1.15,0,1.2)$. Well above T_N at $T=84.2$ K only a broad quasielastic peak is found which appears to be almost independent of temperature, at least between 84.2 and 74.5 K. The dashed line through the 84.2K data is a copy of the dashed line to guide the eye for the 74.5 K scan. As we approach T_N, we see that a narrow elastic peak develops on top of the broad peak. The elastic peak is reminiscent of "central peaks" found near various structural phase transitions. Well below T_N, at $T=30$ K no elastic or quasielastic intensity is observed on the rod, as expected.

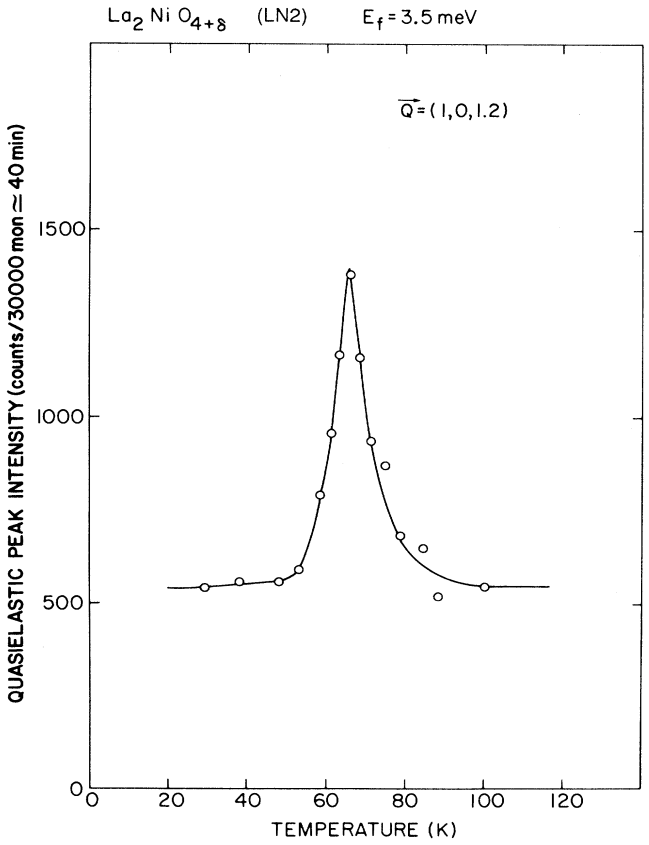

FIG. 7. Peak intensity at $Q=(1,0,1.2)$ and nominal zero-energy transfer as a function of temperature for crystal LN2.

V. MAGNETIC DYNAMICS

To study the magnetic fluctuations in the ordered state of $La_2NiO_{4+\delta}$, we have performed a variety of inelastic constant-Q and constant-$\hbar\omega$ scans for the three single crystals. In Fig. 9, constant-$\hbar\omega$ scans are shown for (a) LN1 ($\delta=0$), (b) LN2 ($\delta=0.067$), and (c) LN3

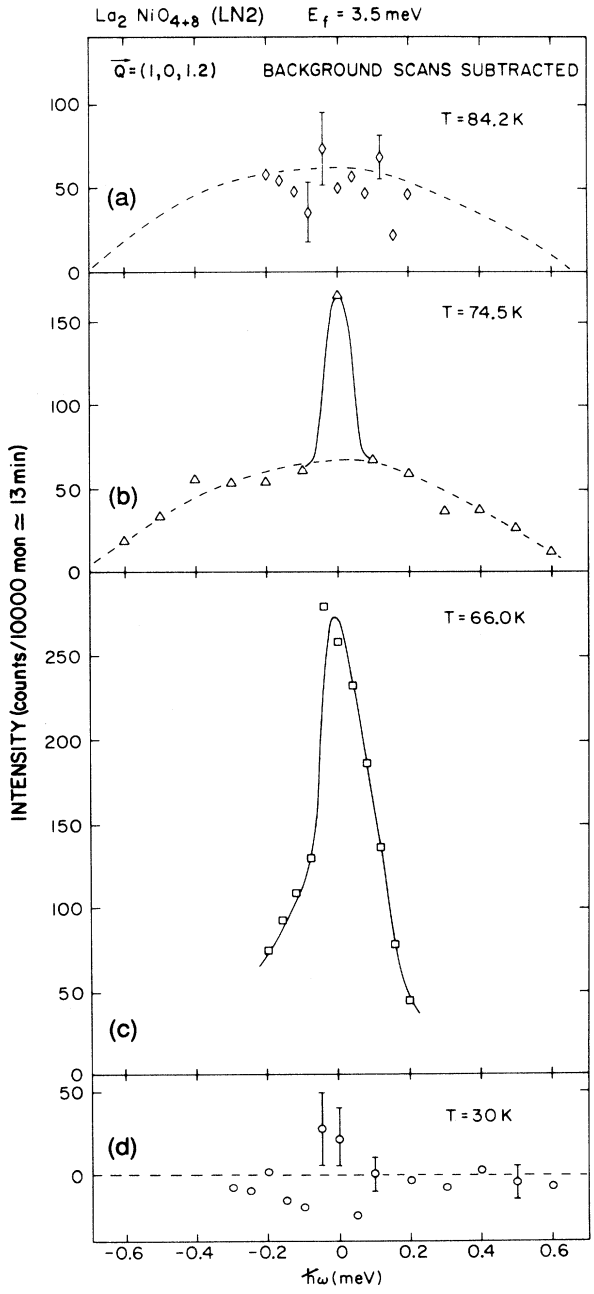

FIG. 8. Energy scans with fixed scattering vector $Q=(1,0,1.2)$ for crystal LN2 at (a) $T=84.2$ K, (b) $T=74.5$ K, (c) $T=66.0$, and (d) $T=30$ K. The quasielastic incoherent background has been subtracted using equivalent scans at $Q=(1.15,0,1.2)$.

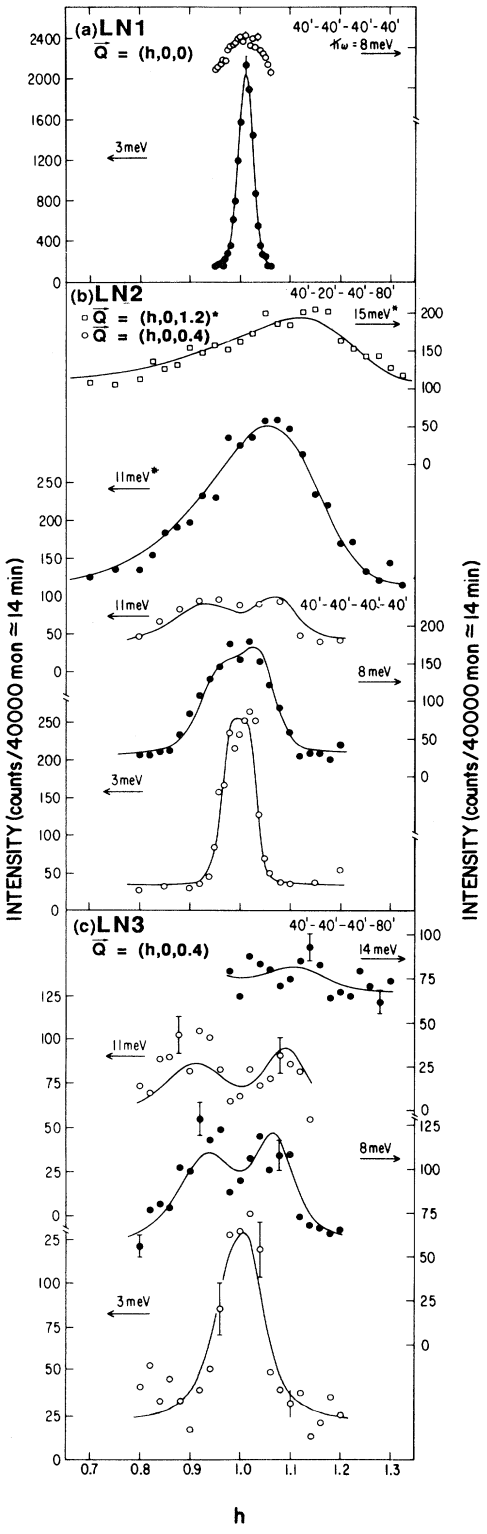

FIG. 9. Constant-$\hbar\omega$ scans for (a) LN1 ($\delta=0$), (b) LN2 ($\delta=0.067$) and (c) LN3 ($\delta=0.077$). The coordinate h represents in-plane momentum transfer in reciprocal-lattice units.

($\delta=0.077$). The coordinate h represents the in-plane momentum transfer in reciprocal-lattice units; as we describe below, the inelastic data are independent of the momentum transfer perpendicular to the basal planes. The data in (a) were taken at room temperature where LN1 is still antiferromagnetically ordered, whereas the data in (b) and (c) are recorded at $T=10$ K, also below the Néel temperatures of the samples in question. The constant energy transfer and spectrometer collimations are noted at or above each set of data. Most of the scans are performed with the final energy fixed at $E_f=13.7$ meV except for the two upper scans in Fig. 7(b), which are taken at $E_f=50$ meV [denoted by an asterisk (*) at the energy transfer]. The data are raw in the sense that no corrections for background have been made.

Conventional antiferromagnetic spin waves are characterized by a linear dispersion relation, $\hbar\omega=cq$, near the antiferromagnetic zone center. For sufficiently large c, $\hbar\omega/c$ will correspond to a reduced wave vector below the resolution limit of the spectrometer. To escape this limit, the best strategy is to increase $\hbar\omega$. Before the spin waves become resolved in the sense implied by a double peak in a constant-$\hbar\omega$ scan, as has indeed been done recently[30] for La_2CuO_4 at $\hbar\omega=0.1$ eV, the constant $\hbar\omega$ scans consist of single peaks somewhat broader than the experimental resolution. Figures 9(a) and 9(b) illustrate this effect. Note that, in (b), the spectra become asymmetric for the largest $\hbar\omega$ because of the focusing effect derived from alignment of the resolution ellipse [in $(\hbar\omega)$-q space] with the dispersion cone on only one side of the antiferromagnetic zone center (see also Fig. 10). To quantify the data and check the consistency of the spin-wave interpretation, a simple analytical expression for the spin-wave scattering was fitted to each scan,

$$S(q,\omega)=A\left[\frac{\Gamma}{(\hbar\omega-cq)^2+\Gamma^2}+\frac{\Gamma}{(\hbar\omega+cq)^2+\Gamma^2}\right]+\mathrm{BG}\ , \tag{1}$$

where A is a scale factor, Γ is the inverse lifetime, c is the spin-wave velocity, q is the distance in Q space from the 2D zone center, and BG is the background. The cross section above was convolved with the spectrometer resolution function, and the parameters adjusted by a least-squares fitting routine to achieve maximum consistency with the data. Values obtained for Γ were all very small, indicating that the spin-wave scattering is resolution limited. The most interesting parameter, the spin-wave velocity, c, was constant for each sample as long as $\hbar\omega>3$ meV, a result which is obvious from the experimental dispersion curves plotted in Fig. 10 [the fitted magnon wave vectors are used to obtain $c(q)$] along with that measured for La_2CuO_4. The curves for the constant energy scans in Fig. 9 with $\hbar\omega>3$ represent the free fits of the cross section in Eq. (1). Due to the limitations of the instrument resolution, the data from the stoichiometric sample LN1 provide only a lower bound for the spin-wave velocity for $\delta=0$. The averaged results from the least-squares fits are $\hbar c\geq 300$ meV Å for $\delta=0$, $\hbar c=130\pm10$ meV Å for $\delta=0.067$, and $\hbar c=98\pm7$ meV Å

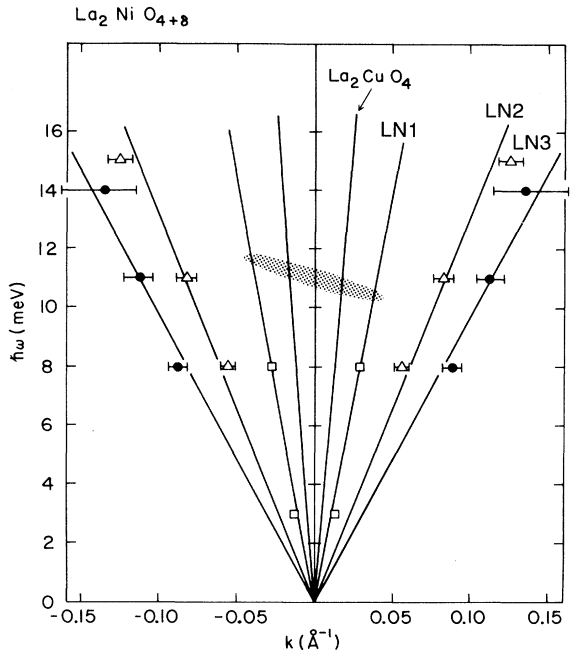

FIG. 10. Experimental spin-wave dispersion curves for LN1, LN2, and LN3. The spin-wave velocity, $c=\omega/q$, decreases rapidly as δ increases. The dispersion curve for La_2CuO_4 obtained from data of Ref. 30 is also included for comparison. The shaded region represents the spectrometer resolution ellipse. Note that the small anisotropy gaps between 0 and 3 meV, as seen in Fig. 11, are *not* included in this figure.

for $\delta=0.077$. For comparison, $\hbar c=850\pm30$ meV Å for nominally stoichiometric La_2CuO_4.[30]

Figure 11 shows constant-**Q** scans for the three $La_2NiO_{4+\delta}$ crystals. At $\mathbf{Q}=(1,0,0)$ and (3,0,0), the spectra have the same shape, but the intensity is lower for the larger of the two magnetically equivalent momentum transfers, see Fig. 11(a). It is therefore safe to conclude that the strong scattering at the ridge is of magnetic origin. As was noted in Ref. 31, the spectra are virtually independent of the component of the momentum transfer along [001], i.e., the fluctuations in the 3D ordered state are mainly of 2D character. The most pronounced features in the constant-**Q** scans are (i) an energy gap, (ii) a peak at the gap energy Δ, (iii) a plateau between Δ and an upper cutoff u. Note that u is beyond the experimental energy range in (a). After the discovery of gaps in $La_2NiO_{4+\delta}$,[31] similar gaps were found for La_2CuO_4.[40] These gaps are all due to anisotropy and can be understood using conventional spin-wave theory. As δ is increased for $La_2NiO_{4+\delta}$, Δ decreases from 3 meV to a value (<1.5 meV) too small to be resolved in the present experiment. In addition to Δ, the cutoff u also decreases with increasing δ, from >10 meV for $\delta=0$ to 6 meV for $\delta=0.077$. This is simply a consequence of the smaller spin-wave velocity at larger δ: as the spin waves become more resolved in q for fixed energy transfers, their contribution to the $q=0$ scattering diminishes.

We have also performed some inelastic polarized beam experiments to determine whether there is any unusual continuum scattering of the type found in mixed valence and heavy-fermion (HF) systems.[41] Figure 12 shows the results for $\delta=0.067$ (LN2). It is apparent that the inelastic spectrum of the inset in (a) is a coarsely resolved version of Fig. 11(b), with no measurable (though note the substantial error bars) magnetic scattering at $\hbar\omega>15$ meV. Also, as expected for conventional antiferromagnets, the spin-flip scattering at the 2D antiferromagnetic [(10l)] zone center has a maximum above T_N [see Fig. 12(b)]. Concommitantly, there is a steady decrease with T in the scattering at the ferromagnetic [(20l)] zone center.

VI. SUMMARY AND DISCUSSION

Table II summarizes our experimental results for comparison with those for $La_2CuO_{4+\delta}$ (all numbers except Δ are from Ref. 30, Δ is from Ref. 40). Whereas Figure 13 shows the magnetic phase diagram of $La_2NiO_{4+\delta}$ for samples made using the procedures described in Ref. 32.

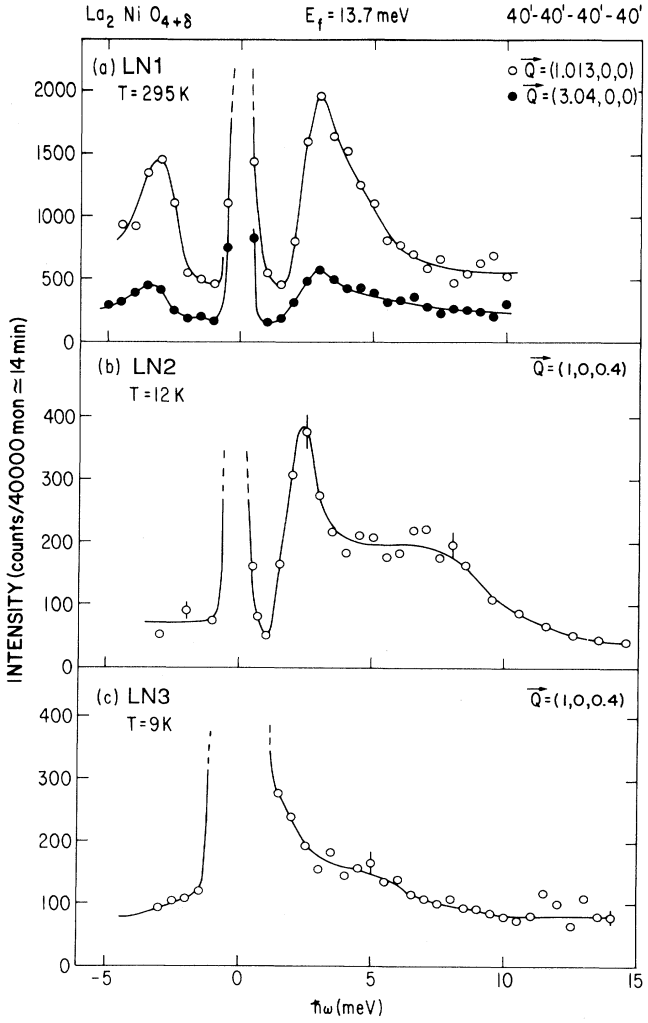

FIG. 11. Constant-Q scans for crystals (a) LN1 ($\delta=0$), (b) LN2 ($\delta=0.067$) and (c) LN3 ($\delta=0.077$) at $T<T_N$.

TABLE II. Measured and fitted parameters for the three $La_2NiO_{4+\delta}$ crystals and the powder specimen are compared with results for $La_2CuO_{4+\delta}$ from Refs. 39 and 41.

Parameter	Unit	Powder specimen $\delta \approx 0.065$	LN1 $\delta = 0.00$	LN2 $\delta = 0.067$	LN3 $\delta = 0.077$	$La_2CuO_{4+\delta}$ $\delta \approx 0$
a	Å (295 K)	3.871(4)	5.473(1)[a]	3.8689(2)	3.8685(2)	5.375(2)
b	Å (295 K)		5.532(1)[a]			5.399(3)
c	Å (295 K)	12.630(5)	12.541(3)[a]	12.6248(7)	12.6353(5)	13.156(4)
T_S	K	220–250	> 300	232–240		> 300
$(b-a)/a_0$	% (10 K)	0.71 (9 K)	1.07 (295 K)[a]	0.74 (10 K)	0.33 (10 K)	0.44 (295 K)
T_N	K	74	> 300	68	49	265
Δ	meV		3	~2	≤1.5	~1.75
c	meV Å		≥300	130±10	98±7	850±30
Moment	μ_B	0.85				

[a]From Ref. 14.

Room-temperature neutron powder diffraction data from stoichiometric La_2NiO_4 are consistent with orthorhombic *Bmab* symmetry. Furthermore, the lattice parameters are in reasonable agreement with values reported in the literature,[13] allowing for slight variations in the absolute oxygen stoichiometry. All nonstoichiometric samples are single-phase tetragonal (*I4/mmm*) at room temperature, within the limits of resolution of the x-ray and neutron data. As δ increases, the **c** parameter increases significantly, whereas basal lattice parameters decrease only very slightly in the tetragonal form. The stoichiometric sample has a significantly larger average basal lattice parameter, after adjusting for the $\sqrt{2}\times\sqrt{2}\times 1$ supercell to obtain $a_T = \sqrt{ab}/2 = 3.891$ Å, than the nonstoichiometric compositions with $a = 3.869$ Å. The tetragonal-to-orthorhombic transition temperature T_S decreases sharply with increasing δ, from ~680 K at $\delta = 0$[16] to <200 K for $\delta = 0.077$. Similarly, the splitting parameter (orthorhombic strain) decreases with increasing δ.

The oxygen-defect concentrations in all of the nonstoichiometric specimens examined in the present study fall within the two-phase coexistence regime

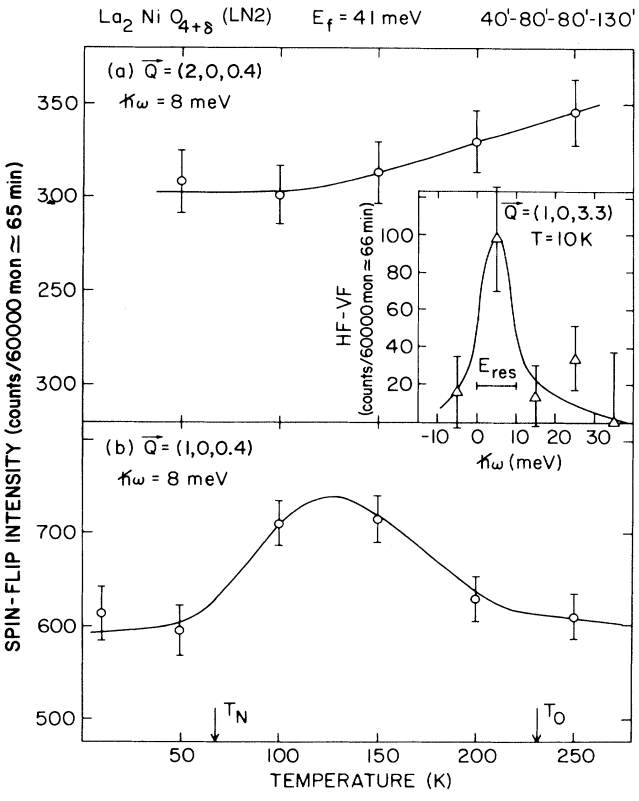

FIG. 12. Temperature dependence of the total spin-flip intensity measured with neutrons polarized parallel to Q (HF) and perpendicular to Q (VF) at (a) $Q=(2,0,0.4)$ and (b) $Q=(1,0,0.4)$ for the $\delta=0.067$ crystal. The inset in (a) shows the difference between horizontal and vertical spin-flip intensities, HF and VF, in constant-$Q=(1,0,3.3)$ scans at 10 K. This difference excludes nonmagnetic scattering due to room background and imperfect beam polarizations (Ref. 42).

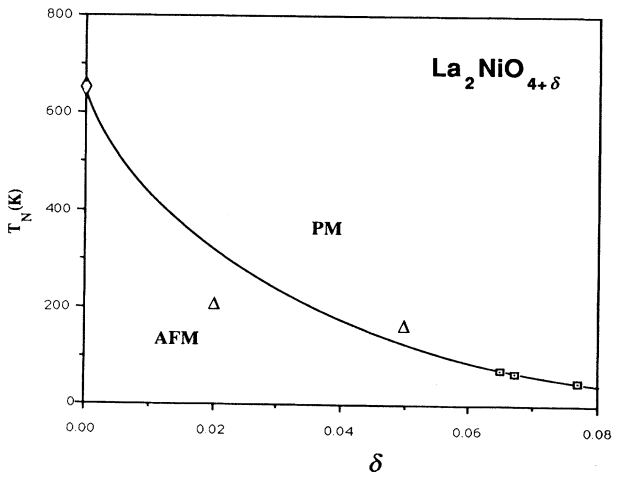

FIG. 13. Magnetic phase diagram for $La_2NiO_{4+\delta}$ prepared and characterized as described in Ref. 32. Experimental Néel temperatures are indicated by symbols: diamond is from Ref. 25, triangles from Ref. 8 (see also Fig. 2 of this paper), and squares from the present neutron-scattering experiments. The solid line provides a guide to the eye.

($0.02<\delta<0.13$) described by Jorgensen *et al.*[13] for $La_2NiO_{4+\delta}$. The two-phase sample they described had an average oxygen excess concentration of $\delta=0.07$, very similar to the values of the nonstoichiometric samples characterized in this investgation. Although structural refinements on our samples lead to agreement factors which are somewhat large (typically 8–12 % for both neutron powder Rietveld and single-crystal x-ray refinements), apparently as a consequence of oxygen-defect correlations, the lattice parameters show no evidence of deviation from tetragonal symmetry or mixed phase composition. This striking inconsistency in phase behavior near $\delta=0.07$ may arise from differing conditions of sample preparation. The nonstoichiometric samples used in this study were obtained "as-grown" from the central region of a 1.4-kg boule of skull-melted material; whereas, Jorgensen *et al.*[13] prepared their two-phase $\delta=0.07$ sample by direct solid-state reaction of the binary oxides in oxygen at high temperature, followed by annealing in nitrogen at 450 °C. Although diffusivity data have not yet been reported for $La_2NiO_{4+\delta}$, it is likely that diffusion rates are low at 450 °C; therefore, it seems possible that either (i) the phase coexistence is due to the onset of phase separation with an upper consolute temperature (T_{uc}) just above 450 °C, such that the time scale for cooling of the skull-melted boule from T_{uc} to room temperature is insufficient to allow phase segregation to progress to a detectable level, or (ii) the kinetics of equilibrium of the sample of Jorgensen *et al.*[13] prevented equilibration of the stable phase at 450 °C under the residual oxygen fugacity of the nitrogen atmosphere. In either case, it is clear that the equilibrium oxygen concentration phase diagram and kinetics of the $La_2NiO_{4+\delta}$ system are poorly understood at present.

The stoichiometric crystal (LN1) has a Néel temperature well above room temperature, as expected on the basis of previous susceptibility studies. T_N falls rapidly with increasing oxygen-defect concentration, such that $T_N<T_S$ for all nonstoichiometric samples studied. Based on susceptibility data, it appears that T_N ($\sim$650 K) (Ref. 25) $<T_S$ ($\sim$680 K) (Ref. 16) in the stoichiometric limit also. For all compositions, the spin structure is colinear with the direction of propagation along [100], parallel to the octahedral rotation axis, as reported earlier.[31] Since the undistorted tetragonal ($I4/mmm$) lattice offers no unique stacking arrangement for the antiferromagnetic sheets, correlations are suppressed by frustration until the structural transition breaks the degeneracy. Below T_N, Ni moments in neighboring Ni-O planes are antiferromagnetically ordered in the more closely spaced (100) planes than in the (010) planes of the orthorhombic cell.

We have determined the magnetic moment of the powder sample ($\delta=0.065$) to be $0.86(5)\mu_B$, which is significantly lower than the value of $1.62(5)\mu_B$ reported by Lander *et al.*[18] for stoichiometric $La_2NiO_{4+\delta}$. Thus, the 3D ordered moment becomes much smaller as δ increased. Similar reductions occur in $La_2CuO_{4+\delta}$ (Refs. 34 and 43) and $La_{2-x}Sr_xCuO_{4+\delta}$ (Ref. 44) with increasing δ and x, respectively. Recent local-spin-density calculations reported by Guo and Temmerman[45] predict that the moment in $La_2NiO_{4+\delta}$ should be sensitively dependent on the extent of octahedral rotation and the ratio of basal and apical Ni—O bond lengths, reflecting variations in hybridization of nickel d states and oxygen p states. However, in the case of the cuprates, the reduction in the 3D ordered moment is not accompanied by an equally large reduction in the frozen *local* moment.[46] This result makes a band-theoretic interpretation less tenable than explanations involving magnetic frustration derived from occasional ferromagnetic superexchange bonds due to holes localized on the planar oxygens.[47] The relevant hypothesis for $La_2CuO_{4+\delta}$, $La_2NiO_{4+\delta}$, and $Pr_2NiO_{4+\delta}$ is that the O^- (instead of O^{2-}) ions in the basal planes are required by charge neutrality, as established assuming that the valences of the lanthanide and transition metal ions are fixed at their $\delta=0$ values.

It is apparent that increasing the oxygen-defect concentration results in a pronounced reduction in both the Néel temperature and the spin-wave velocity. The onset of the tetragonal-orthorhombic transition and the magnitude of the orthorhombic splitting parameter are also sharply reduced. Similar results have been obtained for $La_{2-x}(Sr,Ba)_xCuO_{4+\delta}$ (Refs. 30, 34, 38, 43, and 44) and $Pr_2NiO_{4+\delta}$.[48] Thus in broad outline, the magnetic and structural properties of the layered nickelates differ little from those of the copper oxides. Nonetheless, the existence[49] or absence of superconductivity in layered nickel oxides has not yet been conclusively demonstrated. If the layered nickel oxides are nonsuperconducting, then we conclude that the mechanism for high-T_c superconductivity is either not magnetic, that it involves yet-to-be-established subtleties in the magnetic fluctuations of the cuprates, or that it requires a greater degree of delocalization than that present in the nickelates.

ACKNOWLEDGMENTS

Two of us (D.J.B. and G.A.) are indebted to our colleagues at Brookhaven National Laboratory for their hospitality and for many useful discussions. The work at Brookhaven National Laboratory was supported by the Division of Materials Science, U.S. Department of Energy under Contract No. DE-AC02-CH00016. Support for the work at the University of Delaware was provided by the U.S. National Science Foundation under Contract No. DMR-89-14080.

[1]A. Rabinau and P. Eckerlin, Acta Crystallogr. **11**, 304 (1958).
[2]M. Foëx, A. Mancheron, and M. Líné, Compt. R. **250**, 3027 (1960).
[3]B. Willer and M. Daire, C. R. Acad. Sci. **267**, 1482 (1968).
[4]Hk. Muller-Buschbaum and U. Lehmann, Z. Anorg. Allg. Chem. **447**, 47 (1978).
[5]K. K. Singh, P. Ganguly, and C. N. R. Rao, Mater. Res. Bull. **17**, 493 (1982).
[6]*International Tables for X-ray Crystallography,* edited by T. Hahn (Reidel, Dordrecht, 1987), Vol. A.
[7]C. N. R. Rao, D. J. Buttrey, N. Otsuka, P. Ganguly, H. R. Harrison, C. J. Sandberg, and J. M. Honig, J. Solid State

Chem. **51**, 266 (1984).
[8]D. J. Buttrey, Ph.D. thesis, Purdue University, 1984.
[9]J. M. Honig and D. J. Buttrey, in *Localization and Metal Insulator Transitions,* edited by H. Fritzche and D. Adler (Plenum, New York, 1985), p. 409.
[10]P. Odier, Y. Nigara, J. Coutures, and M. Sayer, J. Solid State Chem. **56**, 32 (1985).
[11]D. J. Buttrey, P. Ganguly, J. M. Honig, C. N. R. Rao, R. R. Schartman, and G. N. Subanna, J. Solid State Chem. **74**, 233 (1988).
[12]P. Odier, M. LeBlanc, and J. Choisnet, Mater. Res. Bull. **21**, 787 (1986).
[13]J. D. Jorgenson, B. Dabrowski, Shiyou Pei, D. R. Richards, and D. G. Hinks, Phys. Rev. B **40**, 2187 (1989).
[14]D. J. Buttrey and A. L. Rheingold (unpublished).
[15]J. D. Jorgensen, B. Dabrowski, Shiyou Pei, D. G. Hinks, L. Soderholm, B. Morosin, J. E. Schirber, E. L. Venturini, and D. S. Ginley, Phys. Rev. B **38**, 11 337 (1988).
[16]C. P. Tavares, Mater. Res. Bull. **20**, 979 (1985).
[17]J. Rodríguez-Carvajal, J. L. Martinez, J. Pannetier, and R. Saez-Puche, Phys. Rev. B **38**, 7148 (1988).
[18]G. H. Lander, P. J. Brown, J. Spalek, and J. M. Honig, Phys. Rev. B **40**, 4463 (1989).
[19]L. Pintschovius, J.-M. Bassat, P. Odier, F. Gervais, B. Hennion, and W. Reichardt, Europhys. Lett. **5**, 247 (1988).
[20]P. Böni, J. D. Axe, G. Shirane, R. J. Birgenau, D. R. Gabbe, H. P. Jenssen, M. A. Kastner, C. J. Peters, P. J. Picone, and T. R. Thurston, Phys. Rev. B **38**, 185 (1988).
[21]C. N. R. Rao and G. V. Subba Rao, Phys. Status Solidi **1**, 597 (1970).
[22]P. Ganguly and C. N. R. Rao, Mater. Res. Bull. **8**, 405 (1973).
[23]M. Sayer and P. Odier, J. Solid State Chem. **67**, 26 (1987).
[24]D. J. Buttrey, J. M. Honig, and C. N. R. Rao, J. Solid State Chem. **64**, 287 (1986).
[25]R. R. Schartman and J. M. Honig, Mater. Res. Bull. **24**, 671 (1989).
[26]G. A. Smolenskii, V. M. Yudin, and E. S. Sher, Fiz. Tverd. Tela (Leningrad) **4**, 3350 (1963) [Sov. Phys. Solid State **4**, 2452 (1963)].
[27]P. Ganguly, S. Kollali, and C. N. R. Rao, Magn. Lett. **1**, 107 (1980).
[28]S. W. Cheong *et al.,* Solid State Commun. **65**, 111 (1988).
[29]T. Thio *et al.,* Phys. Rev. B **38**, 905 (1988).
[30]G. Aeppli, S. M. Hayden, H. A. Mook, Z. Fisk, S-W. Cheong, D. Rytz, J. P. Remeika, G. P. Espinosa, and A. S. Cooper, Phys. Rev. Lett. **62**, 2052 (1989).
[31]G. Aeppli and D. J. Buttrey, Phys. Rev. Lett. **61**, 203 (1988).
[32]D. J. Buttrey, H. R. Harrison, J. M. Honig, and R. R. Schartman, J. Solid State Chem. **54**, 407 (1984).
[33]C. Chaillout, S. W. Cheong, Z. Fisk, M. S. Lehmann, M. Marezio, B. Morosin, and J. E. Schirber, Physica C **158**, 183 (1989).
[34]T. Freltoft *et al.,* Phys. Rev. B **36**, 826 (1987).
[35]R. J. Birgeneau, H. J. Guggenheim, and G. Shirane, Phys. Rev. B **1**, 2211 (1970).
[36]D. Vaknin, S. K. Sinha, D. E. Moncton, D. C. Johnston, J. Newsham, C. R. Safinya, and H. King, Phys. Rev. Lett. **58**, 2802 (1987).
[37]H. A. Halperin, J. Phys. Soc. Jpn. **17**, Suppl. BIII, 12 (1962).
[38]G. Shirane *et al.,* Phys. Rev. Lett. **59**, 1613 (1987).
[39]R. J. Birgeneau, J. Skalyo, Jr., and G. Shirane, Phys. Rev. B **3**, 1736 (1971).
[40]C. J. Peters *et al.,* Phys. Rev. B **37**, 9761 (1988).
[41]S. M. Shapiro, C. Stassis, and G. Aeppli, Phys. Rev. Lett. **62**, 94 (1989).
[42]R. M. Moon, T. Riste, and W. C. Koehler, Phys. Rev. **181**, 920 (1969).
[43]K. Yamada *et al.,* Solid State Commun. **64**, 753 (1987).
[44]Y. Endoh *et al.,* Phys. Rev. B **37**, 7443 (1988).
[45]G. Y. Guo and W. M. Temmerman, Phys. Rev. B **40**, 285 (1989).
[46]D. Harshman *et al.,* Phys. Rev. B **38**, 852 (1988); Y. J. Nemura *et al.,* Phys. Rev. Lett. **59**, 1045 (1987).
[47]V. J. Emery, Phys. Rev. Lett. **58**, 2794 (1987); A. Aharony *et al., ibid.* **60**, 1330 (1988).
[48]D. J. Buttrey, J. D. Sullivan, G. Shirane, and K. Yamada, Phys. Rev. B **42**, 3944 (1990).
[49]Z. Kakol, J. Spalek, and J. M. Honig, J. Solid State Chem. **79**, 288 (1989).